2

STRUCTURAL ANALYSIS OF THE HARCOURT BATHOLITH CONTACT AUREOLE

By F. C. Beavis

Department of Geology, University of Melbourne

Abstract

Mapping and analysis of structural elements in the Ordovician greywackes and slates about the Harcourt Batholith have demonstrated the superposition of small folds, and a strain slip cleavage, on the previously folded sediments. The superposed structures, developed during and as a result of intrusion, imply an outward, horizontally directed compression by the magma on the chamber walls. There is no evidence of vertical stresses. Later stresses caused jointing of the granodiorite, as well as faulting.

Introduction

Mapping of Central Victoria by early workers of the Geological Survey of Victoria produced data which suggested an intimate relationship between the structure of the Lower Ordovician sediments and the form of the Harcourt granodiorite batholith. The present work sought, by using the methods of structural analysis, to determine this relationship, and hence the intrusion tectonics. The project was simplified because the early work of the Survey and the later detailed stratigraphic mapping of W. J. Harris and D. E. Thomas had clearly defined the major structural features.

Field work for the current research was restricted to an examination of all the available exposures, where the structural elements were recorded as data for the statistical analysis. Exposures are poor over much of the area so that some gaps remain in the data. Even where good exposures occurred, weathering tended to obscure some of the critical structures, and in many cases, fresh faces had to be cut.

The help of Mr K. Horwood in the translation of German references, and of my wife, both in the field work and in the translation of Italian references, is gratefully acknowledged. The cost of the field work was covered by research grants from the University of Melbourne.

General Geology

The central part of the area studied is occupied by the arcuate batholith of the Harcourt granodiorite. Although no petrological studies were made, it is apparent that the batholith does not represent a single intrusion; rather, it is made up of several small, related intrusions, each with some unique aspects of texture, composition, and structure. The batholith intruded Lower Ordovician greywackes and slates on which it imposed a thermal metamorphism (Beavis 1962). The aureole is continuous around the whole of the batholith, and although locally covered by alluvium, for the most part it stands out as a low but well defined ridge. Except in the Maldon area, and about the Coliban lobe of the batholith, the aureole is about ½ mile wide, with relativcly high grade cordierite hornfels at the contact, grading to spotted slates at the outer margin. At Maldon, the aureole, consisting of very high grade and metasomatised hornfels, is over 1 mile wide. On the Coliban lobe, the aureole is frequently less than ¼ mile wide, and even at the contact the grade of

metamorphism is extremely low. This is of some significance in the assessment of the intrusion tectonics.

Small masses of grandodiorite, separated from the main mass by alluvial flats, occur in the NW. near Lockwood. While these are obviously related to the main batholith, they are not continuous with it below the alluvium, since hornfels has been observed around each.

Intense intrusion of dykes has occurred into both the granodiorite and the sediments. Although the dykes, which range in composition from acid pegmatites and aplites to ultrabasic monchiquites, represent more than one period of intrusive activity, their structural relations with the sediments are uniform; they are almost invariably parallel to the axial planes of folds, and frequently they have been intruded along these planes. The dykes are normally thin, but in the Big Hill-Mt Lockwood sections of the contact, the margin of the batholith is locally occupied by aplite dykes over 500 ft thick, and outcropping over a length of more than 1 mile.

Regional Analysis

Folding

The broad-scale regional analysis has been based largely on the mapping of Harris and Thomas, summarized by Thomas (1939). The Ordovician sediments have been folded into a series of domes and basins; the folds are large anticlinoria and synclinoria, with varying axial plunge. In the vicinity of the Harcourt batholith there is a regional reversal of plunge: N. of the batholith the folds plunge S. at

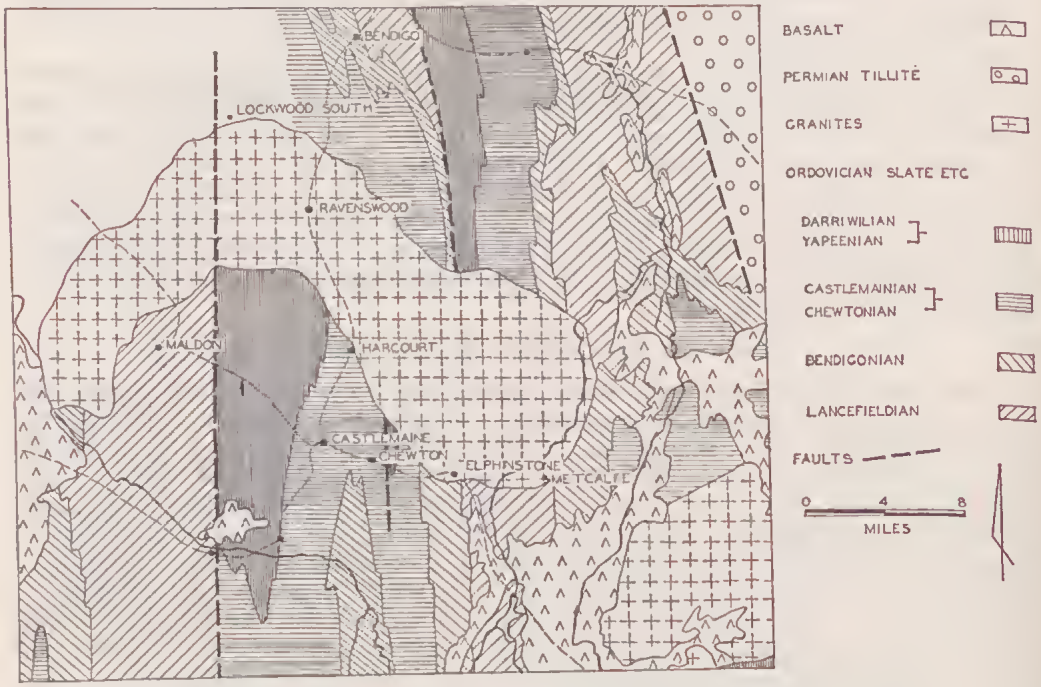

Fig. 1—Regional geological map of Central Victoria, after Harris 1916, and Thomas 1939.

10°-15°, while to the S. of the batholith, plunge is to the N. The batholith therefore occupies an E.-W. axis of plunge reversal, i.e., an open basin structure (which may indicate late collapse of the intrusion). This relationship is comparable to that observed by Stewart (1962) for the Cobaw batholith, which was intruded on the Riddell axis.

Faults and Lineaments

Although many minor faults were recorded, and some evidence of several large faults was observed, only two faults with significance so far as the present research is concerned, occur in the area studied: the Whitelaw Fault, and the Muckleford Fault. The work of Harris (1934) on the former, and of Thomas (1935) on the latter, has shown that while these structures are very old, renewed movement has taken place along them as recently as post-Pliocene times.

Where these faults cut the Ordovician sediments, lithological, palaeontological, and physiographic evidence of movement are clear. In the granodiorite, however, evidence of faulting is much more difficult to find. The E.-facing escarpment on the Whitelaw Fault (due as much to a more resistant lithology as to direct fault displacement) can be traced S. from Bendigo East until it merges with the high terrain of the contact aureole in the Parish of Sedgwick. No equivalent of this escarpment has been observed in the granodiorite; the elevated area about Mt Alexander is the effect of a more resistant granodiorite and has no association with faulting.

Within the batholith there are virtually no exposures on the line of the Whitelaw Fault, but there is a lineament, weakly defined by Myrtle Ck. At the head of this creek, the granodiorite is well exposed in a belt extending from Granite Hill to Mt Alexander. Within this belt there is no evidence of faulting, and it has been concluded that the Whitelaw Fault does not transect the batholith.

In the Chewton area, Harris (1916) postulated faulting from palaeontological evidence. Assessment of the evidence, reinterpreted in the light of the later, more detailed study of the graptolite zones by Harris and Thomas (1938) and the detailed mapping of Chewton by Thomas, raises doubts as to the validity of this structure, which possibly could have been regarded as a southerly continuation of the Whitelaw Fault. It can be stated with some certainty that the Whitelaw Fault pre-dated the intrusion of the batholith; later movement on this fault was the result of stresses with insufficient strength to cause rupture of the granodiorite.

By contrast, considerable evidence that the Muckleford Fault disrupted the granodiorite is available. The physiographic evidence of this fault in the granodiorite is seen in a lineament defined by the headwaters of Muckleford Ck and Spring Ck, and by a low, W.-facing escarpment across which there is a difference in altitude of 200 ft, developed on this lineament, near the Spring Vale Estate. The geological evidence is more impressive. While exposures of granodiorite are poor along the line of the Muckleford Fault, those near Spring Vale are excellent. Here, a very prominent set of N.-S. joints, strongly slickensided, has been developed, and in Spring Ck the granodiorite is locally brecciated. To the N., near Mt Lockwood, the Muckleford Fault locally forms a boundary of the batholith, with low grade brecciated hornfels abutting against the granodiorite, and a thick marginal aplite terminating on the fault. The evidence here indicates a lateral sinistral displacement of 1½ miles. In the S., near Porcupine Flat, a comparable displacement of the contact and of the aureole has been recorded.

The Muckleford Fault transects the batholith; whether or not the initial movement predated intrusion is not clear, but certainly post-intrusive stresses were

adequate to disrupt the granodiorite. Harris and Thomas (1934) and Thomas (1935) have described the Muckleford Fault as a high angle thrust. While no evidence has been found to suggest that this is not so, it is clear that at some stage in the history of the fault there has been a considerable horizontal movement.

Observations in the field, combined with the study of topographic maps of the region, indicate two distinct elements in the stream pattern: a rectilinear element and a curvilinear element. The structural significance of these lineaments might be considerable; Hills (1959), e.g., has suggested that the curvilineament formed by the Coliban R. might reflect ring fracturing. Many of the lineaments are parallel both to the margin of the batholith and to major joint sets. This may be their sole significance, but often there is other evidence that they reflect important structures.

FIG. 2—Lineaments developed on the Harcourt Batholith. The inset shows the distribution of trends of the rectilineaments.

One noteworthy aspect of the streams developed on the granodiorite is that, almost invariably, these streams leave the batholith, and cross the aureole ridge on one of the lineaments. In some cases, as at Lockwood South, Expedition Pass, and Muckleford Ck, the lineament has been proved to represent a fault; in other cases the true nature of the lineament is uncertain or unknown. Some of the lineaments, e.g. that on Bullock Ck, mark important topographic boundaries. E. of Bullock Ck bold continuous outcrops form a rugged landscape, while to the W., the terrain is gently rounded, and exposures are limited to a few isolated boulders. There is some evidence that the Bullock Ck lineament does in fact represent a fault, but this evidence is by no means conclusive.

Mesoscopic Study and Macroscopic Analysis

Granodiorite

Foliation and Lineation

Foliation in the granodiorite is expressed by the preferred orientation of biotite flakes, and is seen in the field as linear traces on joints and other exposed planes. With two exceptions, foliation was observed only in the marginal zone of the batholith, and then only in restricted areas at Ravenswood, Emu Ck, and Porcupine Flat. The foliation observed in the marginal zone was invariably parallel or sub-parallel to the contact; the foliation is to be regarded as a primary flow structure since no evidence of post-crystallization stressing which could develop a foliation in the granodiorite has been obtained. Lineation, also regarded as a primary flow feature, is, with one exception, defined by the orientation of pod-shaped melanocratic schlieren. The exceptional case is the linear arrangement of felspar phenocrysts in a porphyritic phase of the granodiorite near Maldon cemetery. Lineation has an even more restricted development than foliation, only 15 lineations having been recorded for the whole batholith.

Joints

Joints are the most prominent structural elements in the granodiorite. The primary nature of some of the joints is suggested by the occurrence on them of dykes and veins of aplite and pegmatite. Other joints are demonstrably secondary, and the result of shearing stresses, but for most of the joints it is impossible to determine their origin; hence any analysis of the joint pattern must be restricted by this uncertainty.

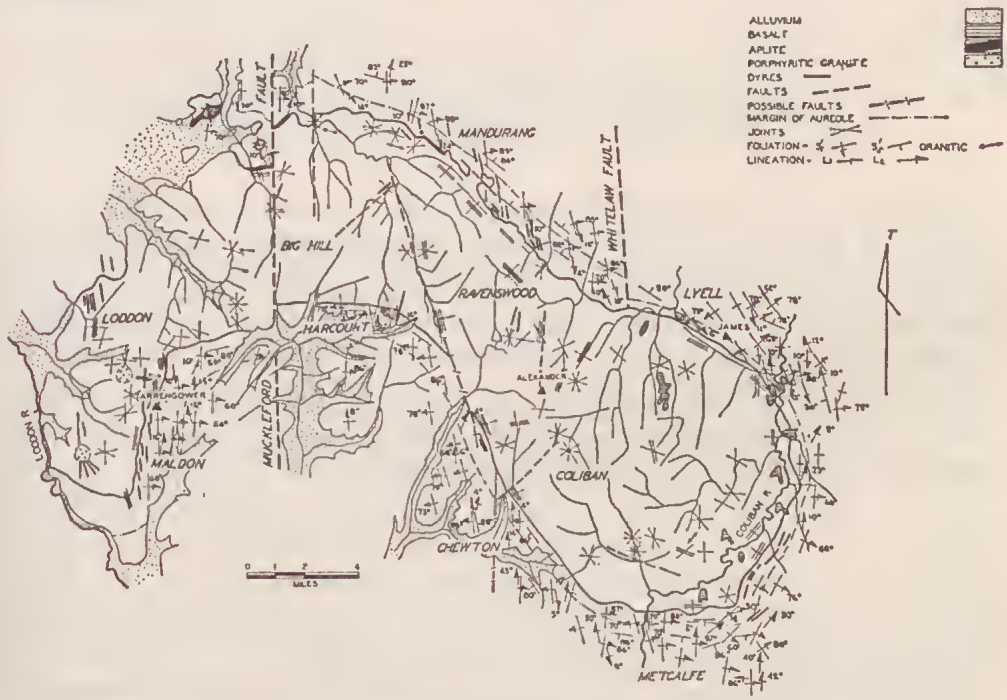

FIG. 3—Structural map of the Harcourt Batholith.

At each exposure examined, vertical joints dominated. Some flat joints occurred, and while many of these are considered to be exfoliation features, some are essential sets of the system. Typical joint systems for most of the exposures are shown on Fig. 3. Many of the joints could be traced only for 20 or 30 ft, others, usually two orthogonal sets, could often be traced for distances of 1 mile or more.

Where quarries have been excavated it was of interest to note that whereas the joint system recorded on the natural surface showed complexity, that exposed in the quarry was usually simple, with two vertical sets. It is most probable that the multiplicity of joints seen in the weathered rock is also a feature of the fresh rock, but that the joints become visible only as a result of weathering and the stress redistribution which would accompany erosional unloading. This relation is shown on Fig. 4b.

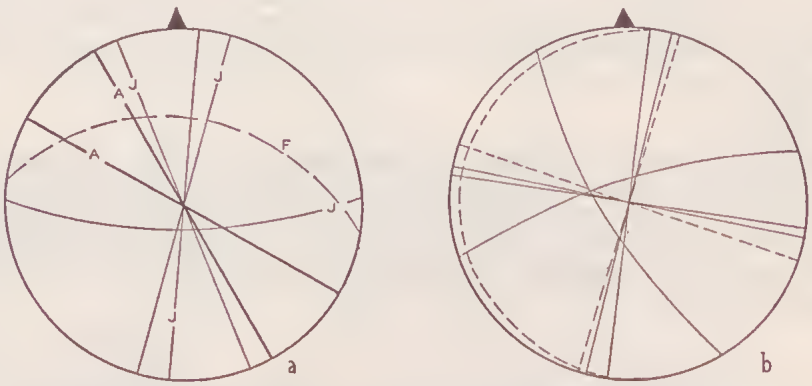

FIG. 4—a. Joints, foliation, and dykes in granodiorite, Belvoir Park. b. Joints at Mt Alexander. Broken lines are joints exposed in the Koala Park quarry; solid lines are joints exposed on the natural surface.

Fig. 4a illustrates a typical joint system. It can be seen that aplite dykes occur on two sets (A). The foliation (F) shows no relationship, apparently, to the jointing. The typical development of steeply dipping joints is seen clearly. One unusual joint system calls for some comment. A flat face of granodiorite, exposed about 1 mile W. from Mt Tarrengower, is broken into polygonal columns by joints, a structure unique in the batholith. It is most likely that this jointing is the result of weathering of a large exfoliated slab.

A multiplicity of joint systems exists within the batholith; however, there is both a local and regional homogeneity of the joint patterns. One of the most outstanding features is the parallelism to the contact of the major joints developed in the marginal zone right around the periphery. This is particularly so between Big Hill and Mt James, and for the full length of the contact of the Coliban lobe. Within the batholith it is possible sometimes to trace major, continuous joints about higher terrain, e.g., Mt Alexander. The high-level, xenolith-free granodiorite of this area has a pronounced set of joints parallel to its margin, suggesting that Mt Alexander comprises a distinct intrusion—an hypothesis which receives some support from petrological evidence (Dr R. J. McLaughlin pers. comm.).

Geometric and kinematic analysis of the granodiorite joint systems is limited by the inability to distinguish certainly between primary structures, and those due to

post-crystallization stresses. Nonetheless, the geometry at almost all of the exposures tends to a uniform four sets, two of which intersect at right angles, and the other two interseeting at 55° to 60°: a typical pattern of fractures due to shearing stress. It is important to note that the two orthogonal sets are the most highly developed.

The joint patterns for the several sectors into which the batholith was somewhat arbitrarily divided for analysis are shown on Fig. 5. It is clear that, throughout, vertical joints predominate, and that the two main sets are those with N./S. and E./W. strike.

Sedimentary Rocks

Foliation

Foliation is used here in a non-genetic sense, and is applied to all planar, penetrative structures. Within the contact aureole, three types of foliation have been formed: bedding (S), slaty cleavage (S_1^1) and strain-slip cleavage (S_2^1). Bedding is the most prominent foliation, with slaty elcavage, restricted to the more incompetent sediments, next in importance. The strain-slip cleavage, too, tends to be restricted to the slates, but the fissuring of sandstones, described by Hills and Thomas (1945) appears in some cases to be a form of this cleavage developed on the hinges of folds during the first deformation, while it has formed also the puckering of slates and the rudimentary boudinage seen in the greywackes. In extreme cases, disruption of puckered laminae by the strain-slip cleavage has produced the cleavage boudinage described by Charlesworth and Evans (1962). Both the slaty and strain-slip clcavages show curvature locally, and on a macroscopic scale. The local curvature is associated with textural gradations in the complexly graded greywackes, as well as with structural discontinuities such as bedding. This is to be regarded as due both to variation in the orientation of the maximum prineipal stress resulting from inhomogeneities in the rocks, and to drag effects from slip along bedding planes during flexural folding. The more general, macroscopic curvature is a reflection of the geometry of the folds.

Lineation

Lineation, parallel to fold axes, is developed in the slates. It is only rarely to be observed in normal exposures, and for the present work most observations were made on freshly cleared faces. The most consistently developed lineation is that due to the intersection of bedding and slaty cleavage. Microcrenulations on bedding planes were less frequent forms. In areas where strain-slip cleavage occurs, quite complex lineations can be seen. Where the bed is planar, with bedding and both strain-slip and slaty cleavages present, three lineations are developed: L1, the intersection of S and S_1^1; L2, the intersection of S and S_2^1; and L2′, the intersection of S_1^1 and S_2^1. Where the superposed deformation is represented by folds as well as strain-slip cleavage, the lineations are complex, and can be interpreted only after the most thorough study (Fig. 6).

Folds

On the mesoscopic seale, the folds are small plunging structures, usually asymmetric, and frequently overturned. The axial planes are almost invariably inclined and curved. The hinge lines may also show some curvature, but this is apparent only on the macroscopic seale; mesoscopically, the hinge lines may be regarded as rectilinear. Geometrically, the folds may be described as plunging, inclined, non-

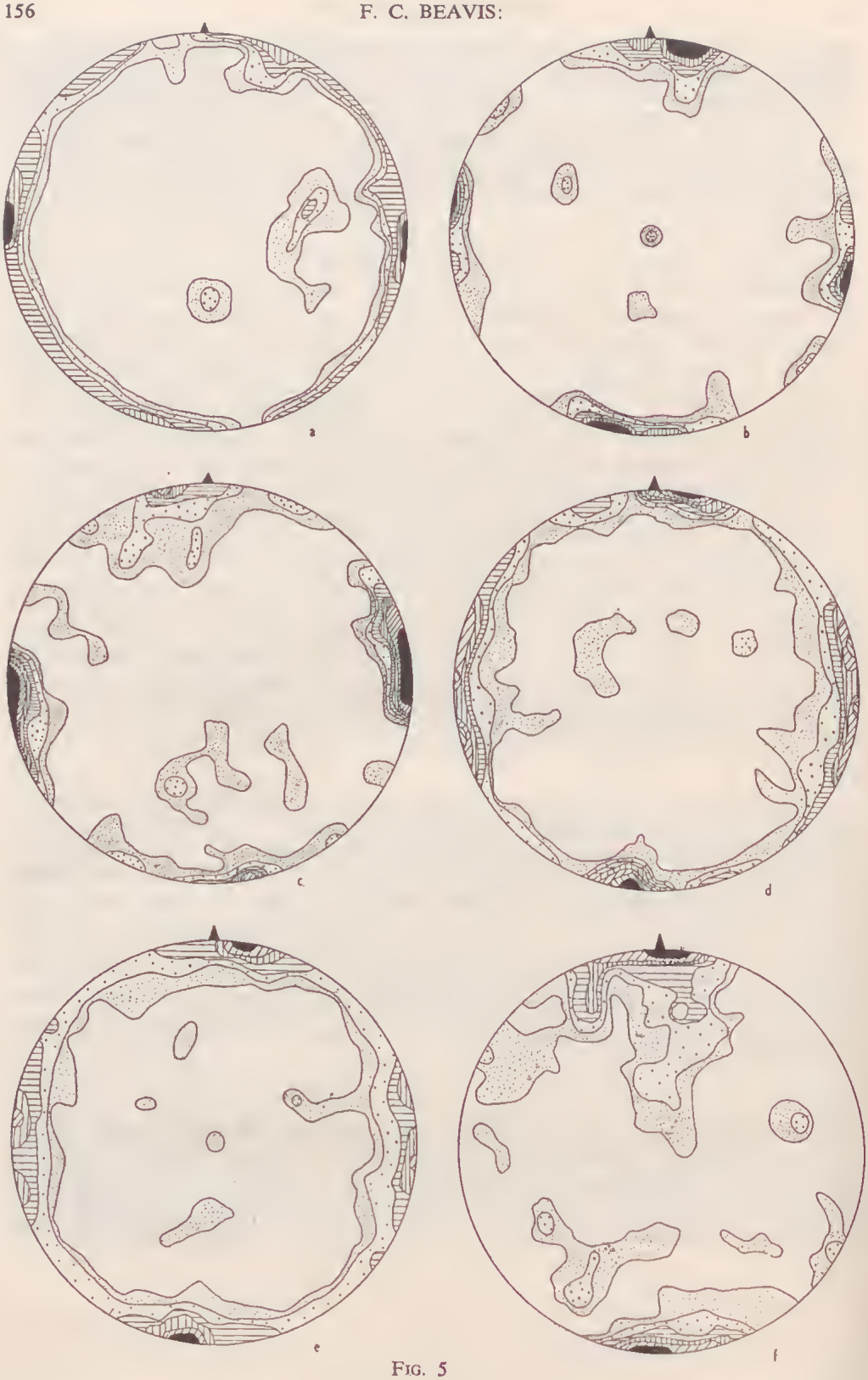

FIG. 5

plane, cyclindrical structures. The strike of the axial plane is rarely parallel to the trend of the axis.

The style of folding is similar. Slate beds show marked thinning on the limbs of the folds, and the folding of these beds has been of the shear type. The greywackes show little or no thinning on the limbs. The folding of these beds has been by flexure, modified to some extent, particularly where complexly graded greywackes have been involved, by shearing. Here the slight thinning of beds on the limbs is the effect of flattening due to shear (Ramsay 1962). The folding of the sediments, from the mesoscopic evidence, has been flexural-shear type; slip along bedding planes has also been a significant feature. While these remarks apply to the first-generation folds, it will be seen that the superposed folds are of the same type, although with much smaller dimensions.

The deformed sediments cannot be described either as B tectonites or as S tectonites, since they have features of each. However, the S tectonite characteristics are dominant. The low degree of metamorphism associated with the folding, and the nature of the tectonite structures developed, suggest deformation at only a moderate tectonic level.

Joints

Because joints are non-penetrative, discrete structural elements, their analysis must be attended by some uncertainty. Various workers, e.g., Turner and Vchhoogen (1960) and Price (1959) have suggested that, since folding has occurred while rocks are in a plastic condition, they cannot be ruptured. However, residual stresses, effective still when the rocks become brittle, would be expected to have the same effects as the original stress; relief of the residual stresses would be marked by the formation of joints. As pointed out by Weiss (1954) and others, it is significant that, in tectonites, the geometrical relationship of joints to penetrative elements of folds is too consistent to be fortuitous.

Of the joints present in the rocks of the Harcourt aureole, the *ac* set are the most important. These joints, interpreted as tension fractures, were rarely truly normal to the B1 lineation. This behaviour has been observed consistently by other workers in other areas. In the Turoka region of Kenya, Weiss (1958) noted a consistent angular relationship between the B axes of folds and the *ac* joints. In the area discussed in the present paper this was also found to be the case statistically, although at individual exposures there is a very wide range. The statistically consistent relationship, combined with the departure of the *ac* joints from truly normal to B, can possibly be explained by the development of a non-uniform stress field late in the deformation history, and the consequent formation of joints normal to variable axes of elastic strain at slight angles to the B axis of the main deformation (Weiss 1958). One interesting aspect of the Harcourt aureole is the fact that the *ac* joints of the sediments are parallel to the major set of the granodiorite.

Fig. 5—Equal area projection of joints in the Harcourt Batholith.
a. Coliban lobe, 200 joints, contours 5-4-3-2-1%.
b. Ravenswood area, 110 joints, contours 5-4-3-2-1%.
c. Big Hill area, 278 joints, contours 7-5-4-3-2-1%.
d. Loddon lobe, 300 joints, contours 7-6-5-4-3-2-1%.
e. Composite diagram for batholith, 888 joints, contours 5-4-3-2-1-½%.
f. Composite diagram for joints in sedimentary rocks about the batholith, 974 joints, contours 4-3-2-1-½-¼%.

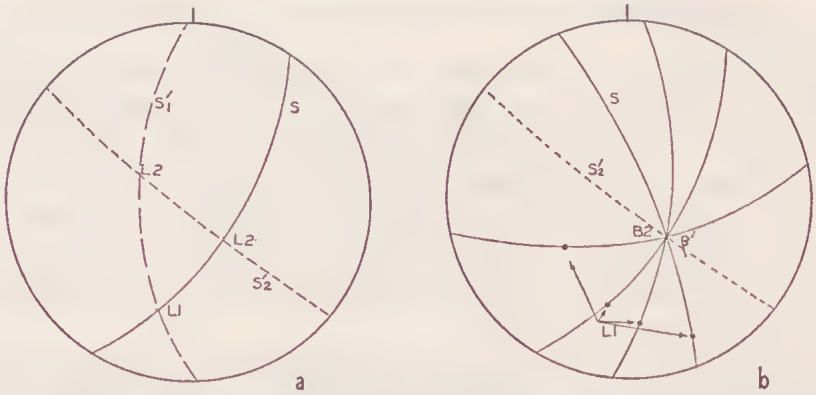

FIG. 6—Lineations developed in tectonites in the Harcourt Aureole.
a. Lineations in planar bed, Coliban R.
b. Lineations in folded bed, Mt James.

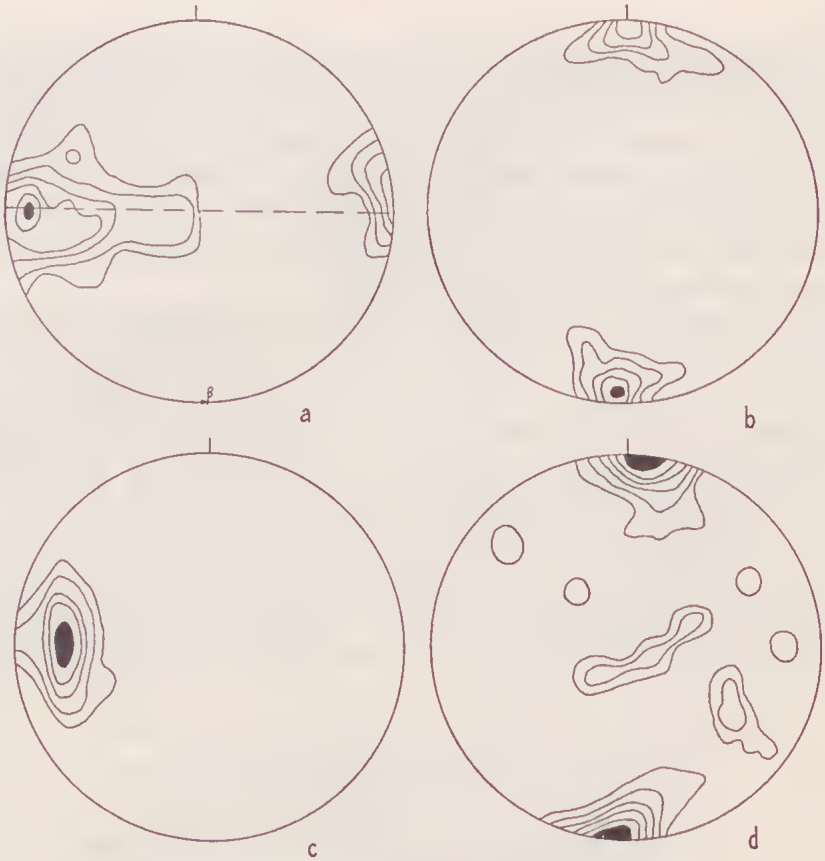

FIG. 7—Geometry of folding, Maldon sub area.
a. 98 π S, contours 6-5-4-3-2-1%.
b. 51B lineations, contours 10-8-6-4-2%.
c. 103 πS_1^1, contours 5-4-3-2-1%.
d. Poles to 175 joints, contours 6-5-4-3-2-1%.

Whereas the *ac* joints cut both the greywackes and slates, *hOl* joints tend to be restricted to the arenaceous sediments. These joints intersect in B of the first deformation, but there is some doubt that all are the result of this deformation since, in the Chewton sub area, these joints in the greywackes pass into strain-slip cleavage in the slates. *hkO* joints are rare, but *Okl* joints are frequently as prominent as the *ac* types. The *Okl* joints intersect in an acute angle which is bisected by the *ac* joint of the system they intersect in *a* and are regarded as shear fractures. *hkl* shear joints were recorded, but are rare.

Macroscopic Analysis

For the purpose of structural analysis, the aureole was divided into sub areas. As analysis proceeded, it became apparent that the folding was not always cylindrical; however, because of the nature of the geometry, this did not affect the validity of the analysis. W. of the batholith, and in the central part of the Barfold Ra., analysis was not possible because of lack of exposures, while to the S. of the Maldon lobe, flooding by the Cairn Curran reservoir prevented any study.

Maldon Sub Area

The folds, previously described by Bradford (1904) and Moon (1897), are cylindrical both on the mesoscopic and macroscopic scales; they are almost invariably asymmetric, and overturned to the W. This is shown in Fig. 7a and 7c where poles to S and S_1^1 form maxima for E.-dipping structures. The geometry has a monoclinic symmetry: there is a single β tautozonal axis parallel to B (Fig. 7b). Strain-slip cleavage is developed, but is invariably parallel to the slaty cleavage. The most striking aspect of the geometry is the parallelism of the fold axial planes to the margin of the batholith.

The joint diagram shows the dominance of *ac* joints, which, statistically, are normal to the B axes. Other joints are only weakly developed.

Harcourt Sub Area

Strain-slip cleavage is strongly developed, with an E.-W. strike and a steep southerly dip, parallel to the margin of the batholith in this area (Fig. 8d). Two quite distinct lineations were observed: one has a maximum for gentle northerly plunge (Fig. 8b) and is coincident with β; the second is formed by the intersection of S_2^1 with S and S_1^1. The geometry is apparently monoclinic, but when all elements are considered, the symmetry is in fact triclinic. The folds tend to be symmetrical, are rarely overturned, and have near vertical axial planes. In this area the *ac* joints, normal to B1, are again the dominant set.

Chewton Sub Area

The S diagram shows a single β, but there is a tendency towards the formation of a second girdle; the symmetry is monoclinic, but has triclinic aspects. In this sub area the slaty cleavage and strain-slip cleavage are sub-parallel, and it was frequently difficult to distinguish between B1 and B2 lineations. The geometry is made more complex by the presence of strain-slip cleavage of two generations. This certainly accounts for the spread in the B1 diagram (Fig. 9b). The B2 lineations are often complex, particularly near the hinges of folds, and where the slaty cleavage is curved. The strain-slip cleavage of the second deformation is once more parallel to the margin of the batholith, but the fold axes and axial planes of the first generation, in contrast to Maldon, are only sub-parallel to the batholith.

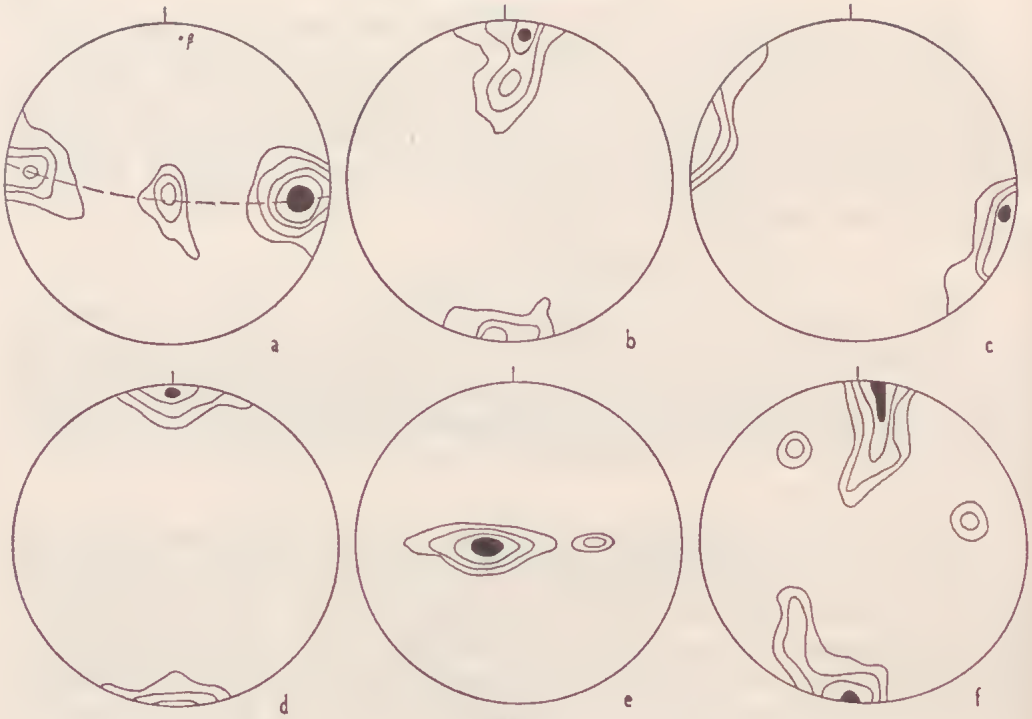

FIG. 8

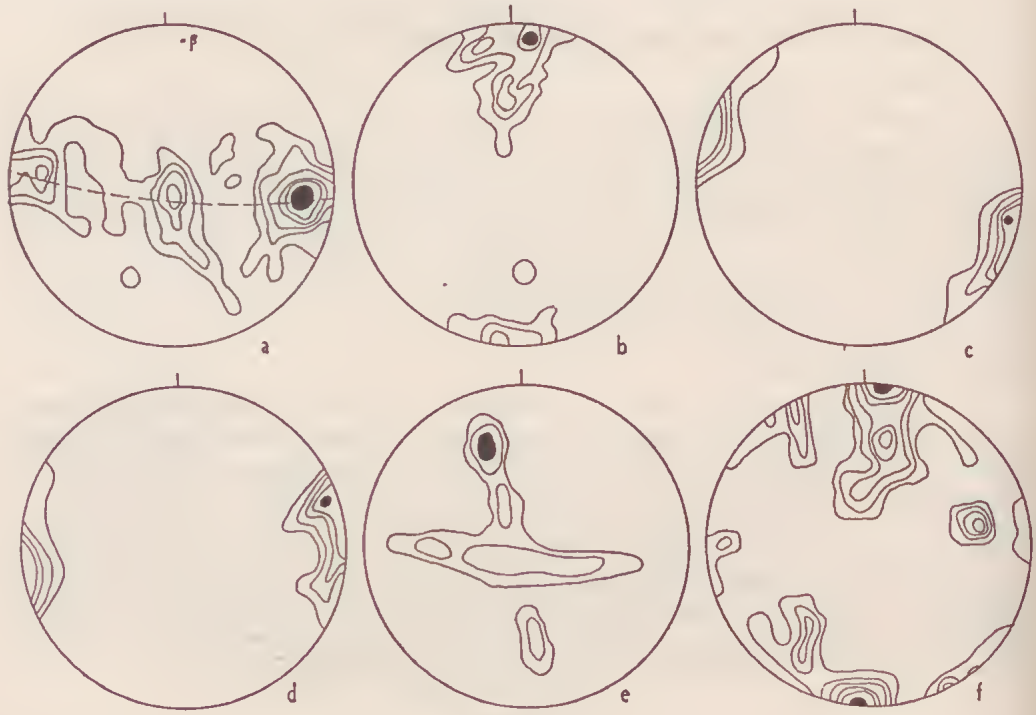

FIG. 9

Folds here, as noted by Thomas (1939, 1940, 1941), Baragwanath (1903) and Dickenson (1941), are uniformly overturned to the E., and overturned isoclinal folding is not uncommon. *ac* joints are still dominant, but in this area, other joints show an increasing importance. In general it was observed near Chewton that fissuring of sandstone was intimately associated with the strain-slip cleavage.

Mandurang Sub Area

The symmetry is apparently monoclinic, but consideration of all the elements again shows triclinicity. There is a single β parallel to B1 (Fig. 10a), which has a gentle plunge to the S. Strain-slip cleavage is parallel to the granodiorite contact, and is vertical. B2 lineations, with near vertical plunge, were clearly distinguishable in the field from B1 lineations. Small folds with axes B2 are commonly observed.

Slaty cleavage, parallel to the axial planes of the folds of the first generation, has a steep easterly dip. The folds are only slightly asymmetric, and are rarely overturned.

Lyell Sub Area

In the contact zone, the metasediments are frequently crumpled and shattered. Here too, superposed folds show the highest development observed in the aureole. These folds are small, with amplitude rarely exceeding 12 inches; the axial planes, defined by strain-slip cleavage, are parallel to the batholith margin. Slaty cleavage shows a more westerly trend than is usual for the region; the two cleavages are sub-parallel, although in some places they intersect in angles as high as 75°. As in most of the other sub areas, the symmetry of S is statistically monoclinic, but that of the fabric as a whole is triclinic.

Metcalfe Sub Area

Between the Lyell and Metcalfe sub areas, too few observations were available for analysis to be attempted. In this intervening region, however, it would seem (Fig. 3) that bedding, slaty cleavage and strain-slip cleavage are all approximately parallel to the granodiorite margin. In the Metcalfe sub area itself, crumpling and shattering of the sediments was again noted near the contact, particularly near the township of Metcalfe. Both bedding and slaty cleavage show a concordance with the batholith: the spread in the diagrams (Fig. 12a, c) is due to the swing in

---

Fig. 8—Geometry of folding, Harcourt sub area.
a. III π S, contours 5-4-3-2-1%.
b. 48 B1 lineations, contours 8-6-4-2%.
c. 52 πS_1^1, contours 8-6-4-2%.
d. 43 πS_2^1, contours 8-6-4-2%.
e. 46 B2 lineations, contours 8-6-4-2%.
f. Poles to 96 joints, contours 4-3-2-1%.

Fig. 9—Geometry of folding, Chewton sub area.
a. 142 π S, contours 6-5-4-3-2-1%.
b. 78 B1 lineations, contours 8-3-2-1%.
c. 97 πS_1^1, contours 5-4-3-2-1%.
d. 73 πS_2^1, contours 5-4-3-2-1%.
e. 54 B2 lineations, contours 8-6-4-2%.
f. Poles to 193 joints, contours 6-5-4-3-2-1%.

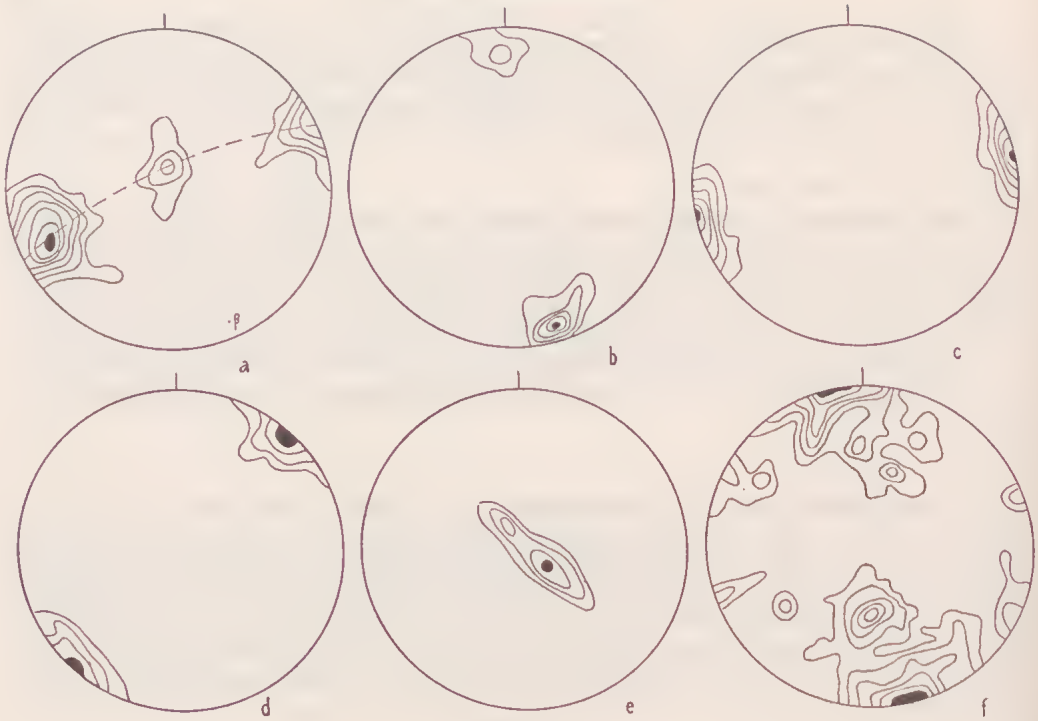

FIG. 10

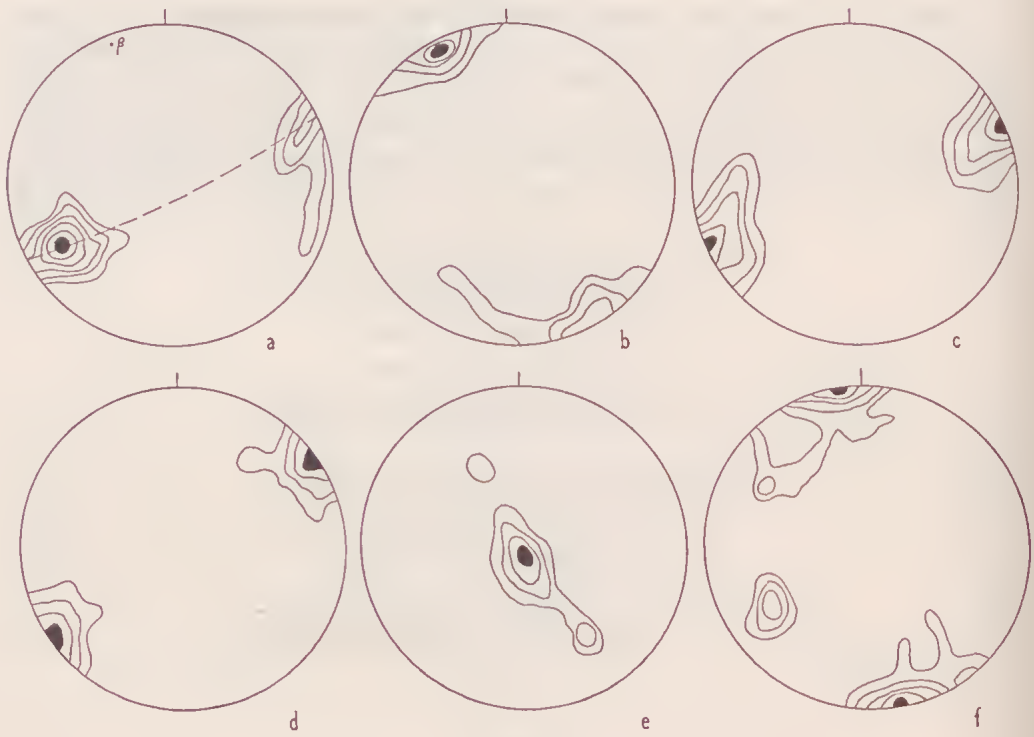

FIG. 11

attitude of these surfaces in the section between Metcalfe and Taradale. In the Metcalfe township area, strain-slip cleavage was not observed, but it is highly developed both south and west of the town, and is parallel to the contact. In this sub-area, a true *a* (of the B1 folds) lineation has been developed in shale beds. This is unique in the aureole.

Quartz Reefs

Fig. 13 shows the orientation of quartz reefs in the contact aureole. These are invariably parallel to the axial planes of the first folds. Some of the reefs show deformation, but this is not typical. The control of emplacement of the reefs was obviously S_1; the strain-slip cleavage has had no apparent influence.

Microscopic Analysis

Granodiorite

Mesoscopic foliation is present in the granodiorite only in the contact zone; elsewhere in the batholith there has been no apparent development of penetrative planar structures. Of the specimens analysed on the microscopic scale, two may be taken as typical. Specimen 1 (Fig. 14a) is a strongly foliated granodiorite from the contact zone at Big Hill. The poles to {001} of biotite form a single maximum normal to the mesoscopic foliation. By contrast, specimen 2 (Fig. 14b) represents a sample of non-foliated granodiorite from Mt Alexander. Three maxima were found for the biotite {001} orientation; this may be due to influences other than flow. There is no evidence of post-crystallization deformation in this rock, and the critical factor would seem to be the homogeneity of the biotite fabric. Three sections cut from the hand sample of specimen 2 gave three distinct orientation patterns for biotite. Homogeneity of fabric does not exist here, and fabric analyses are therefore of no value.

Sedimentary Rocks

Of this group, only the quartz-rich types such as greywacke and quartzite were suitable for microscopic analysis. Attempts were made to determine both quartz and biotite fabrics, but normally biotite was insufficient for reliable study. Most detailed work was therefore carried out on the quartz.

Fig. 15 illustrates biotite {001} fabric in two metagreywackes. These are representative of the two types of biotite fabric found. The symmetry of these fabrics was

---

Fig. 10—Geometry of folding, Mandurang sub area.
a. 209 π S, contours 7-6-5-4-3-2-1%.
b. 96 B1 lineations, contours 5-4-3-2-1%.
c. 103 πS_1^1, contours 5-4-3-2-1%.
d. 56 πS_2^1, contours 8-6-4-2%.
e. 66 B2 lineations, contours 8-6-4-2%.
f. Poles to 201 joints, contours 6-5-4-3-2-1%.

Fig. 11—Geometry of folding, Lyell sub area.
a. 103 π S, contours 6-5-4-3-2-1%.
b. 54 B1 lineations, contours 10-8-6-4-2%.
c. 87 πS_1^1, contours 6-4-3-2-1%.
d. 75 πS_2^1, contours 5-4-3-2%.
e. 46 B2 lineations, contours 8-6-4-2%.
f. Poles to 121 joints, contours 5-4-3-2-1%.

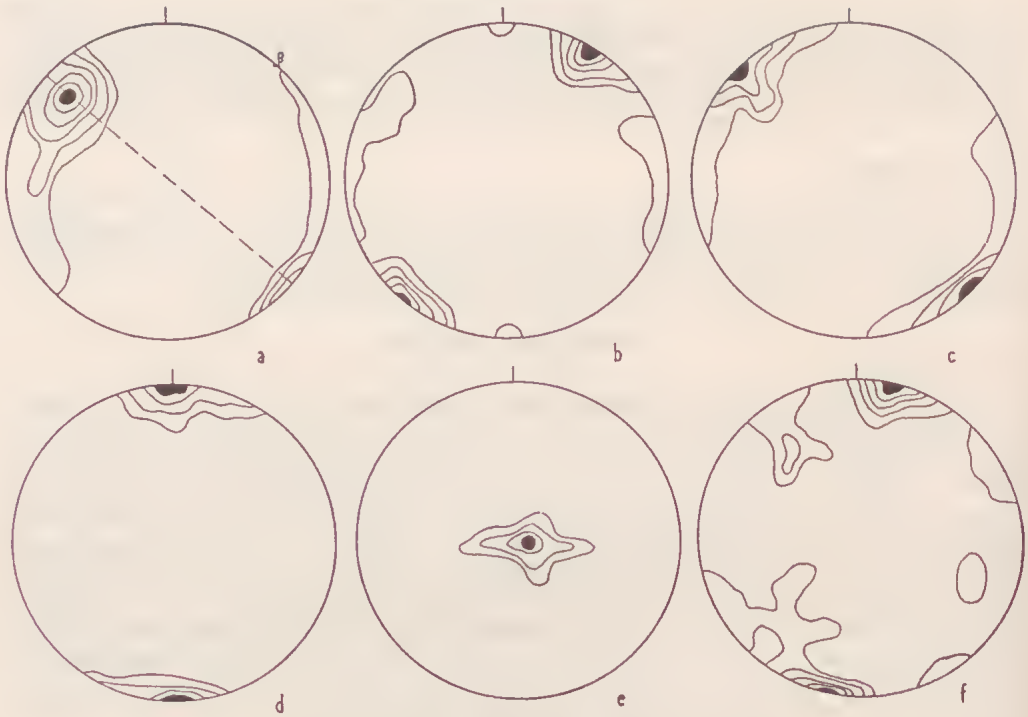

FIG. 12—Geometry of folding, Metcalfe sub area.
a. III S, contours 6-5-4-3-2-1%.
b. 89 B1 lineations, contours 5-4-3-2-1%.
c. 53 S_1^1, contours 8-6-4-2%.
d. 48 S_2^1, contours 8-6-4-2%.
e. 46 B2 lineations, contours 8-6-4-2%.
f. Poles to 178 joints, contours 5-4-3-2-1%.

invariably triclinic; within the fields of both a thin section and a hand specimen, fabric homogeneity was of a high order. Specimen 3 shows one very strong maximum, with two less well developed maxima. The strongest is normal to the mesoscopically visible S^1, while of the two weaker, one is normal to S and the other to S_2^1. Specimen 4 shows one strong maximum which is normal to S_2^1, and one weak maximum normal to S_1^1. There is no apparent parallelism of biotites to S.

The biotite fabrics then give microscopic evidence of the formation of two deformational *s* planes within the sedimentary rocks about the batholith. The biotite fabric appears as the result of two distinct deforming stresses which produced, as inferred from the mesoscopic data, $B \wedge B'$ tectonites.

The quartz fabrics invariably display a triclinic symmetry. The degree of homogeneity of these fabrics varies with scale: it is high on the scale of a thin section (see example Fig. 16). Similarly, for samples taken from a single bed at Lockwood South, a high degree of homogeneity was found. On a regional scale, it would be difficult to assess this feature unless some hundreds of specimens were examined:

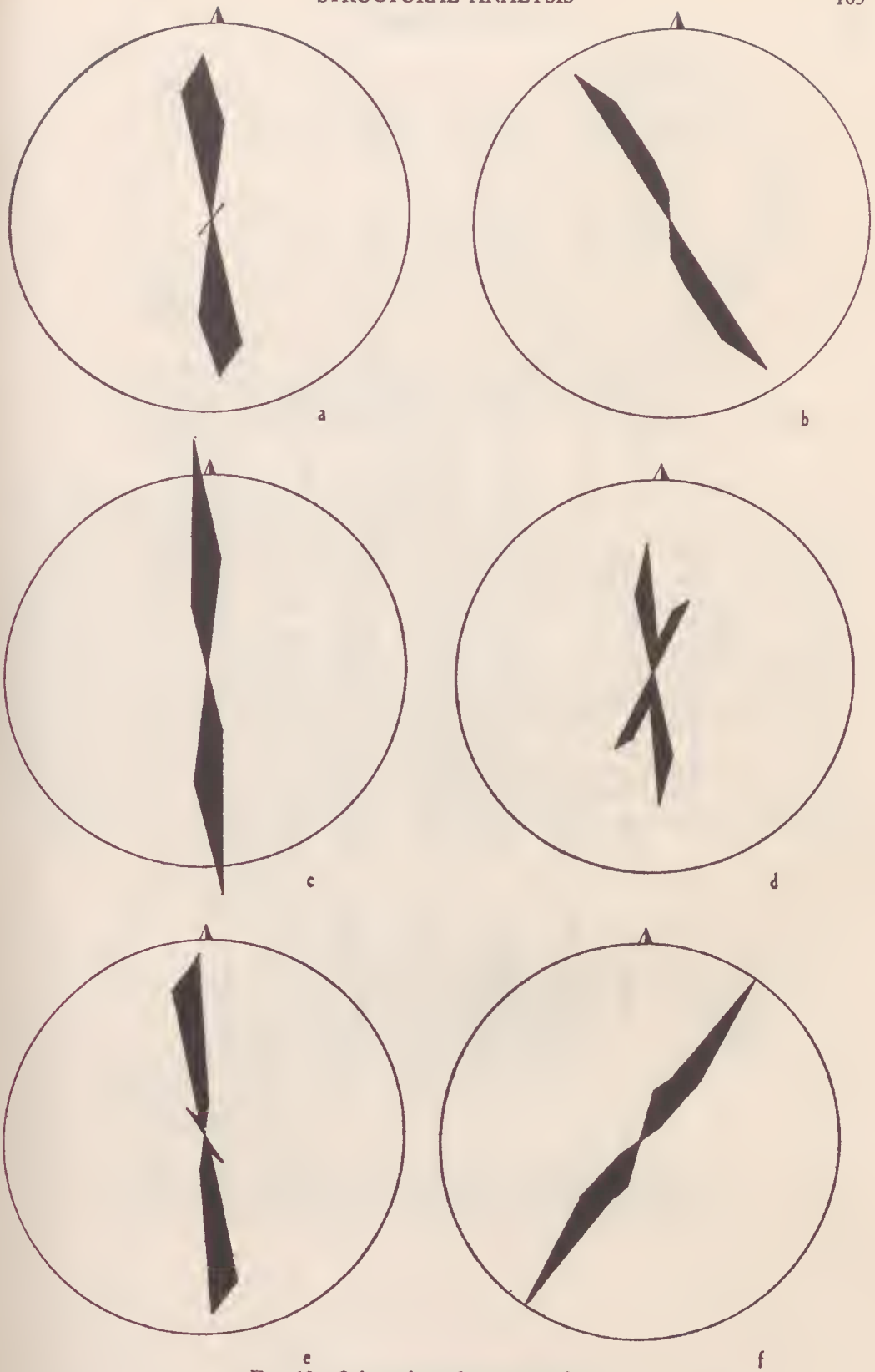

FIG. 13—Orientation of quartz reefs.
a. Chewton, b. Lyell, c. Maldon, d. Barfold Ranges, e. Mandurang f. Metcalfe.

TABLE 1

Summary of Macroscopic Geometry

Sub Area	Bedding, S	Cleavage S_1^1	Cleavage S_2^1	Lineations	Total Symmetry	Trend of margin of Batholith
Maldon	Cylindrically folded; β plunges 0°/N. Monoclinic	Dip 62°E. Strike N.-S.	—	B1 plunges 8°S.	Monoclinic	N.10°E.
Harcourt	Cylindrically folded; β plunges 8°/N.6° E. Monoclinic	Dip 78°W. Strike N.11°E.	Dip 85°S. Strike E.-W.	B1 plunges 10°N.8°E. B2 plunges 75°W.	Triclinic	E.-W.
Chewton	Cylindrically folded; β plunges 10°/N.60°E. Monoclinic-Triclinic	Dip 80°W. Strike N.12°E.	Dip 80°W. Strike N.17°W.	B1 dispersed 10° plunge, N.6°E. B2 dispersed 32° plunge N.20°W.	Triclinic	N.25°W.
Lyell	Cylindrically folded; β plunges 6°/N.20°W. Monoclinic	Dip 90° Strike N.22°W.	Dip 90° Strike N.32°W.	B1 plunges 10°N.20°W. B2 plunges 85°S.45°E.	Triclinic	N.40°W.
Metcalfe	Cylindrically folded; β plunges 0°/N.43°E. Monoclinic	Dip 90° Strike N.43°E.	Dip 90° Strike E.-W.	B1 plunges 0°N.43°E. B2 plunges 85°E.	Triclinic	E.-W.
Mandurang	Cylindrically folded; β plunges 11°/S.24°E. Monoclinic	Dip 90° Strike N.10°W.	Dip 90° Strike N.46°W.	B1 plunges 10°S.24°E. B2 plunges (i) 75°/S.48°E. (ii) 75°/N.42°W.	Triclinic	N.45°W.

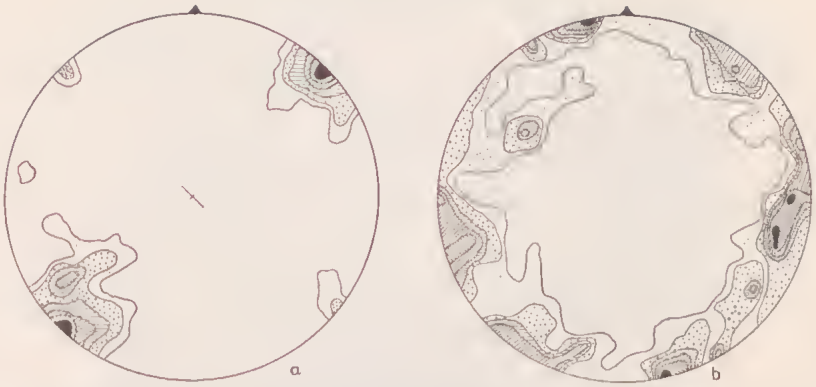

FIG. 14—Poles to {001} of biotite in granodiorite.
a. Big Hill contact zone, foliated granodiorite, 300 poles, contours 6-5-4-3-2-1%.
b. Non-foliated granodiorite, Mt Alexander Koala Park quarry. 300 poles, contours 6-5-4-3-2-1%.

in the region studied, the few samples suggest that the quartz [0001] fabric is regionally inhomogeneous.

Axial distribution analyses (A.V.A.) were carried out on three specimens. A.V.A. are used to distinguish between orientation patterns which are due to inhomogeneities in the fabric field as a whole, and those which are due to inhomogeneities between individual grains without reference to the complete fabric field (Case I and Case II, respectively of Sander 1950). Orientation patterns of case I show maxima in the diagrams which may be referred to specific S planes within the rock, since the orientation pattern is determined by the mechanical behaviour of the whole rock. For case II, the grains may show a strong preferred orientation, but grains with a given orientation are not spatially related to definite S planes in the fabric: this is known as direction homogeneity.

Of the three specimens analysed in this way, No. 5 is a metagreywacke from Mt Herbert; No. 6, a metaquartzite from Lockwood South; and No. 7, a metaquartzite from S. of Harcourt. Each of these rocks differs in the proportion of quartz

FIG. 15—Poles to {001} of biotite in two metagreywackes.
a. Specimen 3, Big Hill Tunnel, 300 poles, contours 6-5-4-3-2-1%.
b. Specimen 4, Barfold Ra., 300 poles, contours 7-6-5-4-3-2-1%,

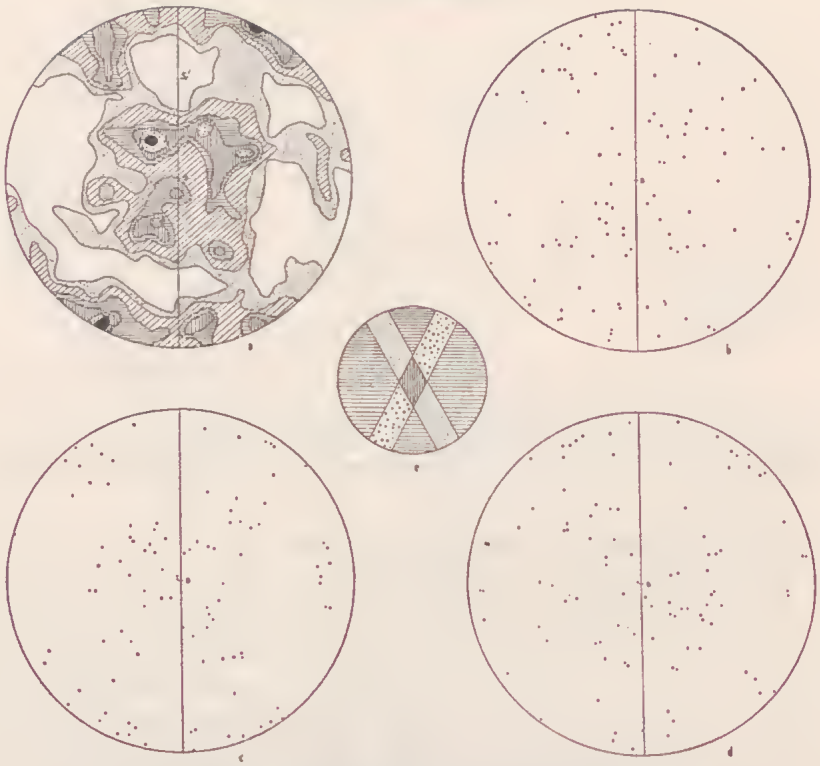

FIG. 16—A.V.A. of metagreywacke, Mt Herbert Specimen 5.
a. 491 [0001] quartz. Contours 5-4-3-2-1-½%.
b, c, d. Partial diagrams for [0001] of 100 grains.
e. Key to shading of grains in figure 17.

present, and together represents the main types of quartz-rich metasediments in the aureole.

Examinations of faces cut on a hand specimen of the metagreywacke (No. 5) suggested the existence of three sets of planes: the mesoscopic S_1^1 (aB1), and two *hOl s* planes which intersected in B1, and symmetrically disposed about S~. The [0001] quartz orientation diagram (Fig. 16a) measured in the *ac* plane of the fabric, shows a strong maximum in *b* (B1), and an equally strong maximum near *a* (possibly to be regarded as B2) of the fabric. Minor maxima also occur, the overall diagram suggesting *hOl* girdles. The symmetry is triclinic.

Partial diagrams, prepared for different areas of the thin section, confirm the homogeneity of the quartz fabric. Fig. 17a, a tracing of the photomicrograph of the section, shows that grains contributing to each of the maxima of the orientation diagram (direction groups) show no obvious mutual differences in spatial relationships. There seems to be a slight tendency for the grains to be aligned in the *hOl* planes, but it is possible that this alignment is fortuitous, and direction homogeneity may be inferred. It is clear also that grains forming each of the direction groups show no mutual differences in dimensions.

As a further investigation of direction homogeneity, the centres of the grains of each direction group were plotted as points; the distribution of points was measured, and the diagrams contoured (Fig. 17b, c). These show that while direction homogeneity is not perfectly achieved, it is closely approximated.

In specimen 6, a metaquartzite, with quartz constituting 93 per cent of the rock, bedding was visible as colour bands; two well developed sets of shear planes were also visible. Tests similar to those for No. 5 proved homogeneity of the [0001] quartz fabric. The symmetry of this fabric is triclinic. The [0001] quartz orienta-

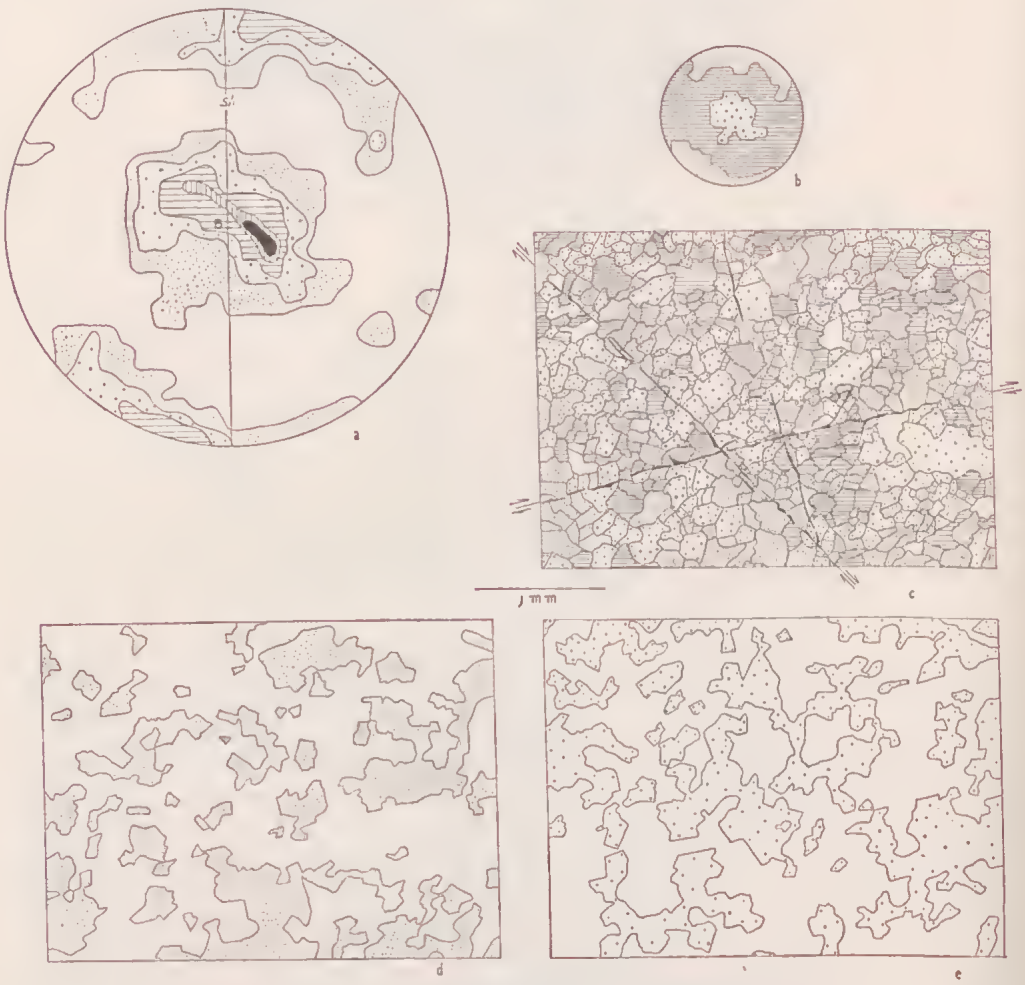

FIG. 18—A.V.A. metaquartzite, specimen 6.

a. 473 [0001] quartz. Contours 5-4-3-2-1%.
b. Key to grains in Fig. 18c.
c. Tracing of photomicrograph of specimen 6, with grains shaded according to orientation.
d. Domains of grains of the direction group indicated by fine stippling in 18c.
e. Domains of grains of the direction group indicated by coarse stippling in 18c.

tion diagram (Fig. 18a) measured in the *ac* plane of the fabric, has a strong maximum in B1, but in contrast to No. 5, there is no development of *hOl* girdles, nor of a maximum in or near *a*.

In Fig. 18c it can be seen that the grains show some tendency to lie in planes, but as in specimen 5, direction homogeneity appears to be approximated. For this analysis, the grains forming the two main direction groups were separated by tracing from Fig. 18c. In both cases, the grains form large, somewhat irregular domains which clearly define the *hOl* planes. Direction homogeneity is less than in No. 5. The shear planes are clearly expressions of post-recrystallization deformation; while there is a tendency for these planes to follow grain boundaries, they frequently cut through grains. Displacement, the direction and amount of which are measurable, has occurred along these planes, but there has not been a significant rotation. The three sets apparently developed synchronously.

Specimen 7 is a metaquartzite in which quartz constitutes 75 per cent of the rock. Neither the thin section nor the hand specimen shows clearly any planar dis-

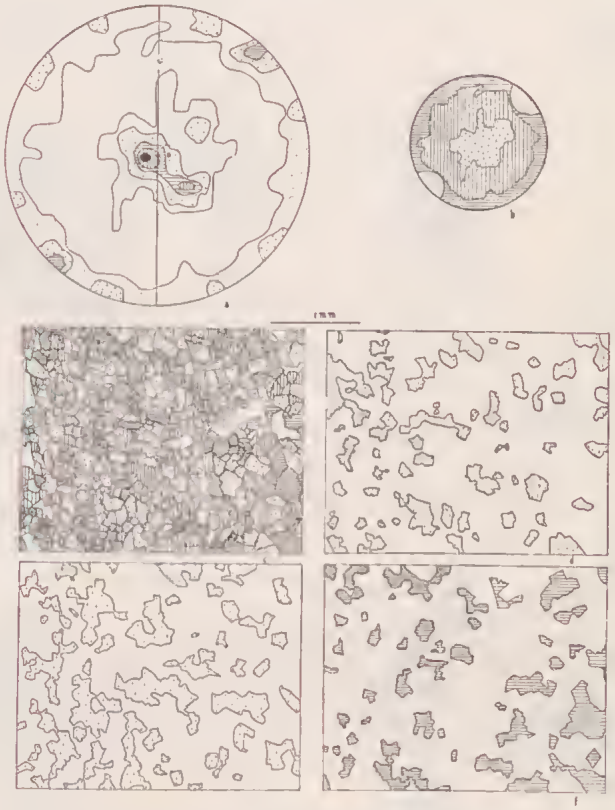

FIG. 19—A.V.A. of metaquartzite, specimen 7.
a. 565 [0001] quartz. Contours 5-4-3-2-1%.
b. Key to shading Fig. 19c-19f.
c. Tracing of photomicrograph of specimen 7.
d. Domains of direction group shown by fine stippling in (c).
e. Domains of grains shown by coarse stippling in (c).
f. Domains of grains shown by horizontal lines in (c).

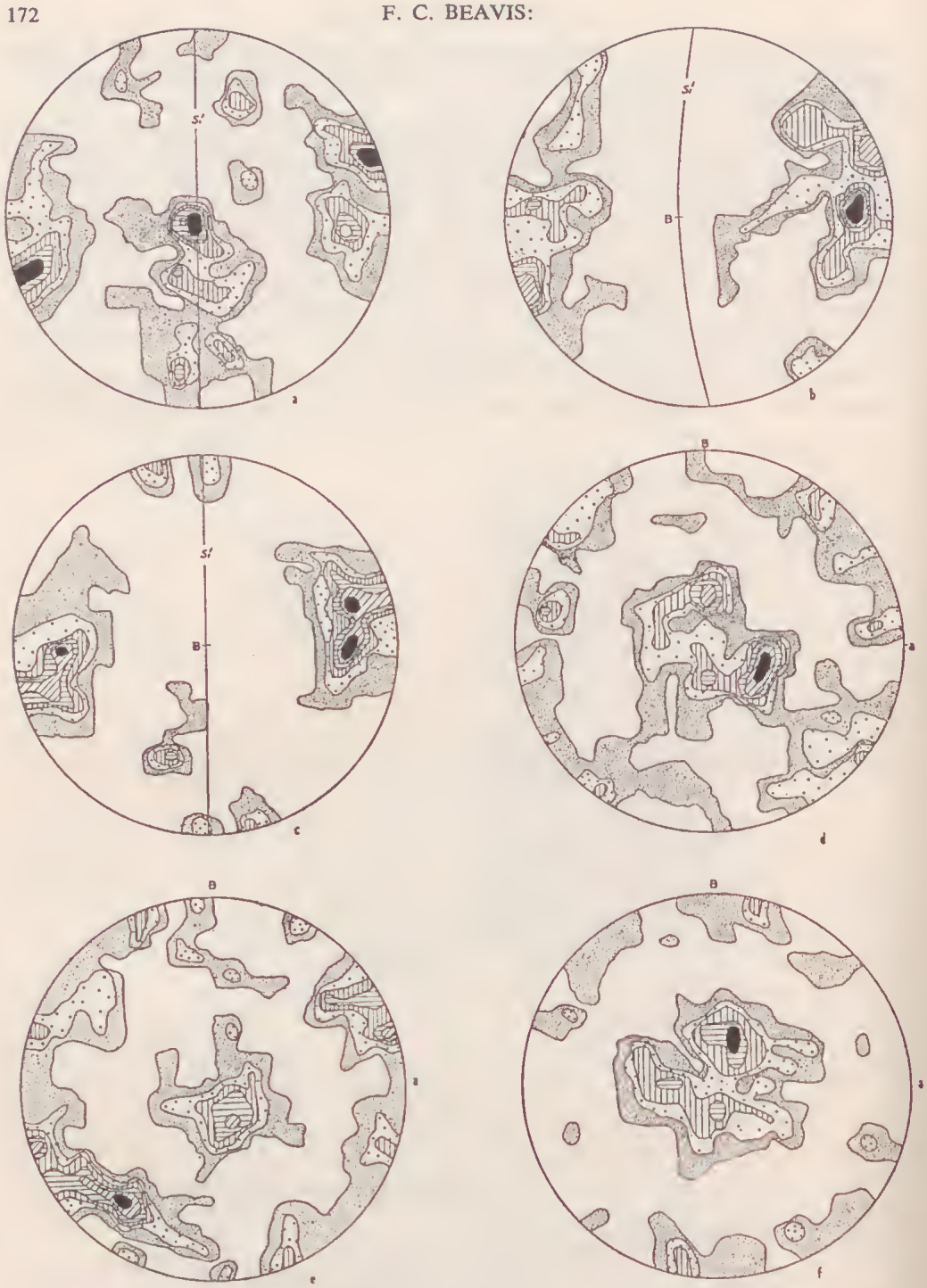

FIG. 20—[0001] quartz diagrams.

a. Specimen 8, Chewton. *ac* plane, 300 [0001] quartz contours 5-4-3-2-1%.
b. Specimen 9, Barfold Ra. *ac* plane, 300 [0001] quartz contours 6-5-4-3-2-1%.
c. Specimen 10, Big Hill. *ac* plane, 300 [000] quartz, contours 6-5-4-3-2-1%.
d. Specimen 11, Lockwood South, *aB*1 plane, 300 [0001] quartz, contours 6-5-4-3-2-1%.
e. Specimen 12, Maldon, *aB*1 plane, 300 [0001] quartz, contours 6-5-4-3-2-1%.
f. Specimen 13, Fogarty's Gap, *aB*1 plane, 300 [0001] quartz, contours 5-4-3-2-1%.

continuity, although Fig. 19c suggests some orientation of the grains in aB1 and *hOl* shears. The [0001] orientation diagram shows features intermediate between those of the two previous specimens. In common with these, a strong maximum is present near B, and as in No. 5 there is an *ac* girdle, although this lacks the maximal concentration in *a* shown by No. 5. Fabric homogeneity was established by partial diagrams; the symmetry of this fabric is triclinic.

The separation of the domains of each of the three direction groups suggests that direction homogeneity is of a low order, and that this specimen approaches case I of Sander. The grains form small irregular domains, which for each group tend to define planar discontinuities of a particular set.

Six specimens were analysed to establish the [0001] quartz fabric without recourse to the detailed A.V.A.

The diagram for specimen 8 (Fig. 20a), a greywacke, shows a maximum in B (B1), with weaker maxima in *c*. *hkO* girdles show some development. Specimen 9 is a slightly sheared metagreywacke, and specimen 10, an intensely sheared metagreywacke. The fabric of these specimens (Fig. 20b, c) differs from that of others already discussed in that the maximum in B is absent. In No. 9 there is a maximum in *c* and a tendency to an *ac* girdle; in specimen 10 two maxima of equal intensity occur symmetrically disposed with respect to aB, and lie on *hOl* planes defined by partial girdles, an orientation reflecting the influence of flattening.

In specimen 11 (Fig. 20d), a metaquartzite, *hkl* girdles and maxima near *c* have been developed. There is also some evidence of an aB girdle comparable to that of No. 8. A quartzite from near Maldon, specimen 12 (Fig. 20e) shows an aB girdle, with maximal concentrations near *c* and in a partial *hkl* girdle. A similar rock at Fogarty's Gap, No. 13 shows a concentration of [0001] about *c*, with only partial *hkl* and aB girdles.

In all of the rocks examined, the quartz grains were notably free of deformation features: undulatory extinction was noted only occasionally, and deformation lamellae in only 6 grains. In general, it is clear that both the quartz and biotite fabrics are due to more than one set of stresses. Post-folding deformation, which imposed a strain-slip cleavage on the slates, has clearly influenced the orientation of both the biotite and quartz in the arenaceous rocks. Post-recrystallization deformation is indicated by shear planes, but this deformation does not appear substantially to have influenced the microfabric except in a few rare cases. One of the most significant facts is that the microfabric, like the macrofabric, has a markedly triclinic symmetry.

Discussion

In the region surrounding the Harcourt batholith the rocks are clearly B $\wedge$ B′ tectonites, the geometry of which is triclinic. The original folding of the sediments, which predated the emplacement of the batholith, produced, in a very general manner, monoclinic B $\perp$ B′ fabrics; on this has been overprinted the fabric of a later deformation. The following is a summary of the results of analysis at all scales.

1. The axis of the batholith is arcuate, and has a general E.-W. trend, convex to the N. The E. lobe of the batholith has a circular margin; around this lobe the aureole is much thinner than elsewhere, and the grade of the contact rocks is much lower.
2. The arcuate axis of the batholith more or less coincides with an E.-W. axis

of downfolding in the Ordovician sediments, i.e. the batholith may be associated with a collapse structure.

3. Where the margin of the batholith is meridional or sub-meridional, the bedding is parallel to the contact (Maldon, Barfold Ra.) or subparallel to the contact (Chewton). In the Barfold Ra. sharp departures occur from the regional trend.

4. Regionally, the axial planes of folds (S_1^1) have a NNW. trend with steep easterly dip. In the region between Maldon and Chewton, polycinal folding has been developed: in the Chewton area axial planes S_1^1 dip 70°-80°W., in the Maldon area they dip 60°-70°E., while in the intervening area they tend to be vertical.

5. Everywhere the sediments were studied in the aureole, a strain-slip cleavage, parallel to the margin of the batholith, and locally, superposed folds with axial planes defined by the strain-slip cleavage, have been developed.

6. Petrofabric data give evidence of multiple deformation.

7. Petrological studies (Beavis 1962) showed a retrograde aspect of the contact metamorphism, suggesting the development of stresses during or, less probably, after recrystallization.

It may be concluded that two main deformations have been responsible for the development of the present structure of the metasediments in the Hareourt aureole. The first was a tangential E.-W. compression, affecting the whole of Central Victoria, and predating intrusion; the second was effective only about the batholith. Because of the orientation of the structures resulting from this later deformation, it is to be concluded that the stress was everywhere normal to the margin of the batholith, and hence that intrusion was markedly an outward acting compression by the magma. That this deformation was synchronous with the intrusion is demonstrated by the nature of the thermal metamorphism (Beavis op. cit.); the metasediments show aspects of stressing, but there is no evidence of post-recrystallization deformation of intensity sufficient to lead to mineralogical changes. Such a stress field would account not only for the mesoscopic superposed structures noted, but also for the macroscopic polyclinal folding developed between the two lobes of the batholith, where opposing stresses would have acted. It would also account for curvature of beds and axial planes on the east margin of the Coliban lobe. It is important to note that no evidence of vertical stresses was obtained. This is somewhat puzzling, since such stresses would be expected.

The mechanics of intrusion were possibly more complex than has been determined here. It is likely that the batholith consists of a number of intrusions, and for the Coliban lobe at least, some ring fracturing and collapse may have occurred. This is suggested both by the circular form of the contact, and the thinness and low grade of the aureole here. If collapse of the magma occurred it is not unlikely that the inner part of the aureole was involved.

One important aspect remains to be considered: the jointing both of the sediments and of the granodiorite. Analysis of the former shows that these were the result of stresses of the first deformation, and appear to have been only slightly modified by the second deformation. Some anomalous joints in the sediments may have formed during the later stressing, but these are rare. Many of the joints in the granodiorite are certainly primary, but, as was pointed out, some are clearly secondary, and the result of shear stresses. If the assumption that the joint pattern of the granodiorite is due to shearing is valid, then an E.-W. tangential compression,

post dating intrusion, must have occurred. Microfabric data give some evidence of this, while such a stress would be necessary for the fracturing of the granodiorite along the Muckleford Fault. Such a stress, since it would be parallel to the original folding stress, would have little influence on the jointing of the metasediments.

References

Baragwanath, W., 1903. The Castlemaine goldfield. *Mem. Geol. Surv. Vict.* 2.

Beavis, F. C., 1962. Contact metamorphism at Big Hill. *Proc. Roy. Soc. Vict.* 75 (1): 89-100.

Bradford, W., 1904. The Maldon goldfield. *Bull. Geol. Surv. Vict.* 14: 1-28.

Charlesworth, H. A. K., and Evans, C. K., 1962. Cleavage boudinage. *Geol. Mijn.* 41 (8): 356-362.

Dickenson, D. R., 1941. Structural conditions at the Nimrod workings. *Min. Geol. J. Vict.* 4 (2): 225-227.

Harris, W. J., 1916. The palaeontological sequence in the Castlemaine district. *Proc. Roy. Soc. Vict.* 29 (1): 50-74.

————, 1934. The eastern boundary of the Bendigo goldfield. ibid. 46 (2): 200-206.

Harris, W. J., and Thomas, D. E., 1933. The geological structure of Eastern Talbot. ibid. 46 (2): 153-178.

————, — ————, 1938. A revised classification . . . of the Ordovician rocks. *Min. Geol. J. Vict.* 1 (3): 62-72.

Hills, E. S., 1959. Cauldron subsidences. *Geol. Runds.* B57H3: 543-561.

Hills, E. S., and Thomas, D. E., 1945. Fissuring in sandstones. *Econ. Geol.* 40: 51-61.

Moon, R. A., 1897. Report on the Maldon goldfield. *Mines Dept. Vict. Special Report.*

Price, N. J., 1959. Mechanics of jointing. *Geol. Mag.* 96: 149-167.

Ramsay, J. G., 1962. The geometry . . . of similar type folds. *J. Geol.* 70 (3): 309-327.

Sander, B., 1950. *Einfuhrung in die Gefugekunde.* J. Springer, Wien. II: 161-217.

Stewart, A., 1960. Unpublished thesis, University of Melbourne.

Thomas, D. E., 1935. The Muckleford Fault. *Proc. Roy. Soc. Vict.* 47 (2): 213-229.

————, 1939. The Chewton Mine. *Min. Geol. J. Vict.* 2 (1): 11-14.

————, 1939. The structure of Victoria. ibid. 1 (4): 59-64.

————, 1940. Notes on the Chewton goldfield. ibid. 2 (2): 91-97.

————, 1941. Reefs at Wattle Gully. ibid. 2 (4): 219-224.

Weiss, L. E., 1954. A study of tectonic style. *Univ. Calif. Publ. Geol. Sci.* 30 (1): 1-102.

————, 1958. Structural analysis at Turoka, Kenya. *Overseas Geol. and Min. Res.* 7 (1): 3-35; 7 (2): 123-153.